Weld Discontinuities in Austenitic Stainless Steel Sheets—Effect of Impurities and Solidification Mode

Sulfur is a detrimental element, causing both hot cracks and pore-like discontinuities, while phosphorus and solidification mode mainly affect hot cracking

BY V. P. KUJANPÄÄ

ABSTRACT. Nineteen Type 316 austenitic stainless steel sheets were welded using autogenous gas tungsten arc welding. Different kinds of discontinuities were formed in the welds, *i.e.*, cracks, center cavities, cracked center cavities, ripple cavities, and undercuts. Compared to the primary ferritic mode, the primary austenitic solidification mode augmented both cracking and ripple cavity formation. The incidence of center cavities, cracked center cavities and undercuts was not affected by the solidification mode.

Sulfur played an important role in discontinuity formation, and cracks and cavities could be eliminated by reducing its content to below 0.003%. Phosphorus had the same kind of effect on cracking but not on the formation of the other types of defect. The reasons for the effects of the solidification mode and impurities are explored, and the practical importance of the results is also considered.

Introduction

Austenitic stainless steel sheets and tubes with a material thickness of 1 to 3 mm (0.04 to 0.12 in) are generally gas tungsten arc welded (GTAW) using single or multiple electrodes. They are often regarded as exhibiting good weldability, and only joint penetration variation is seen as a troublesome problem (Ref. 1). This is basically true, where no high expectations for productivity or quality requirements are laid down. With mechanization and automation, however, the increasing demand for higher welding speeds has also highlighted a problem of discontinuity formation in sheet welding.

The effect of welding conditions on discontinuity formation was studied in a previous paper (Ref. 2), the discontinuities being classified into six types according to their size, shape and location in the weld. It was stated that cracks and ripple cavities could be formed at low welding speeds typical of single-electrode GTAW, while center cavities, undercuts and humps were found at high speeds typical of multiple-electrode GTAW.

The mode of solidification of austenitic stainless steel welds is essentially dependent on the weld metal composition, *i.e.*, the concentration of austenite and ferrite-forming elements. This can be identified on the basis of the microstructure or the weld metal composition. The solidification mode is primary austenitic, if the ratio of chromium and nickel equivalents[1] is below a certain value, about 1.5; or the solidification mode is primary ferritic if it is over that value (Ref. 3). Cooling conditions have only a minor effect on solidification mode. The boundary between the primary austenitic and primary ferritic modes is 1.50 in GTAW at a welding speed 100 mm/min (4 ipm) and about 1.55 in GTAW at a speed 800 mm/min (30 ipm) (Ref. 4).

Solidification mode and impurities play a prominent role in hot cracking and microfissuring in welds associated with massive constructions composed of austenitic stainless steels (Refs. 7–9). Welds are found to be susceptible to solidification cracking, if they solidify in a primary austenitic mode and contain a normal amount of impurities. On the other hand, those solidifying in primary ferritic mode or having a very low impurity content ($P + S < 0.01\%$) are not susceptible (Ref 8). Very little is known, however, of the importance of the solidification mode and impurities for the formation of cracks and other kinds of discontinuities in sheet and tube welding, especially when high welding speeds are used. It is simply recognized in practice that the maximum applicable welding speed varies greatly, even between heats of the same type of steel.

This paper is a part of an extensive study dealing with the formation of GTAW weld discontinuities in austenitic stainless steel sheets and tubes. The purpose here is to demonstrate the importance of the solidification mode and the impurities, sulfur and phosphorus.

Experimental Procedure

Materials

The test materials were selected from

Paper presented at the 64th Annual AWS Convention in Philadelphia, Pennsylvania, during April 24-29, 1983.

V. P. KUJANPÄÄ is a Research Fellow, University of Oulu, Laboratory of Physical Metallurgy, Oulu, Finland.

[1]*From among the various equivalents presented in the literature, those given by Hammar and Svensson (Ref. 5) were used, because they provide the best correlation between composition and solidification mode (Ref. 6):* $Cr_{eq} = \%Cr + 1.37\%\ Mo + 1.5\%\ Si + 2\%\ Nb + 3\%\ Ti$; $Ni_{eq} = \%Ni + 0.31\%\ Mn + 22\%\ C + 14.2\%\ N + \%Cu$

Table 1—Compositions (wt-%) and Calculated Ratios of Chromium and Nickel Equivalents for Test Sheets

Test sheet no.	C	Si	Mn	P	S	Cr	Ni	Mo	Cu	N	Nb	Ti	Cr_{eq}	Ni_{eq}	Cr_{eq}/Ni_{eq}
1	.047	.36	1.36	.031	.003	17.3	13.3	2.61	.22	.043	.00	.04	21.5	15.6	1.38
2	.041	.46	1.42	.006	.001	17.0	13.0	2.71	.17	.055	.00	.00	21.4	15.3	1.40
3	.041	.43	1.33	.006	.020	16.8	12.8	2.70	.16	.056	.00	.00	21.1	15.1	1.40
4	.019	.45	1.37	.032	.016	17.2	13.3	2.65	.24	.038	.00	.05	21.6	14.9	1.45
5	.028	.49	1.68	.035	.016	17.3	12.7	2.58	.16	.061	.00	.00	21.6	14.9	1.45
6	.023	.41	1.72	.034	.017	17.3	12.7	2.56	.15	.058	.00	.00	21.4	14.7	1.46
7	.025	.49	1.54	.034	.015	17.2	12.9	2.70	.17	.030	.00	.00	21.6	14.5	1.49
8	.035	.48	1.47	.029	.001	16.7	12.2	2.50	.13	.020	.00	.01	20.9	13.8	1.51
9	.046	.46	1.63	.035	.120	17.1	10.7	2.13	.18	.089	.00	.00	20.7	13.7	1.52
10	.044	.41	1.72	.036	.010	16.8	11.1	2.63	.20	.061	.00	.00	21.0	13.7	1.54
11	.026	.53	1.69	.031	.003	16.8	11.9	2.70	.18	.049	.00	.02	21.4	13.9	1.54
12	.025	.54	1.73	.037	.010	17.4	12.5	2.66	.26	.023	.00	.00	21.9	14.2	1.54
13	.038	.49	1.64	.035	.004	16.7	11.5	2.67	.23	.023	.00	.00	21.1	13.4	1.57
14	.049	.56	1.57	.029	.017	17.1	11.4	2.63	.17	.014	.00	.00	21.5	13.5	1.59
15	.031	.47	1.80	.033	.017	16.9	11.2	2.66	.18	.044	.00	.00	21.2	13.2	1.60
16	.039	.62	1.70	.038	.016	16.7	10.7	2.59	.15	.067	.00	.00	21.2	13.2	1.61
17	.042	.50	1.59	.039	.020	16.7	10.9	2.63	.14	.043	.00	.00	21.1	13.1	1.61
18	.032	.51	1.53	.028	.001	16.7	11.3	2.81	.19	.037	.00	.00	21.3	13.2	1.62
19	.031	.46	1.42	.006	.001	16.7	10.7	2.70	.17	.049	.00	.00	21.1	12.7	1.66

Type 316 austenitic stainless steel sheets on the basis of their weld metal impurity content and solidification mode. The compositions of the nineteen sheets used in the tests are presented in Table 1. The ratio of chromium (Cr) and nickel (Ni) equivalents varied within the limits of Cr_{eq}/Ni_{eq} = 1.38 to 1.66 and impurities within the limits S = 0.001–0.12% and P = 0.006–0.038%.

All materials were commercial grades from six producers except for sheets 2, 3 and 19, which were rolled laboratory melts. The sheet thickness was always 2 mm (0.08 in.).

Test Procedure

Mechanized GTA single electrode welding was used for all test welds. The bead-on-sheet welds were produced autogenously, without a groove, with the specimen fastened to a rigid jig. A detailed description of the procedure has been presented in the literature (Ref. 2) where the reproducibility of the test results is also discussed.

Two welding speeds – 200 and 800 mm/min (8 and 31 ipm) – were used for each sheet. They were selected on the basis of published information (Ref. 2) so that cracks should be formed at the lower speed and center cavities and undercuts at the higher one. The welding current was as high as possible, just avoiding hole formation. This was done in order to get a maximum number of discontinuities. Due to the different welded joint penetration properties of the sheets, this meant that the current varied from sheet to sheet – between 140 to 180 A and 230 to 260 A at speeds of 200 and 800 mm/min (8 and 31 ipm), respectively. Otherwise the conditions were kept constant as shown in Table 2.

Metallographical Methods

The test welds were pickled in a solution of 15% HNO_3 + 5% HF and cleaned. They were examined visually by stereo-light microscope and by x-ray radiography (acceleration voltage 90 kV, current 5 mA, exposure time 15 to 21 min).

The number, length and depth of the weld discontinuities on the weld and root faces and on the x-ray film were measured by stereo-light microscopy. The microstructure of the welds was also examined by using conventional light microscopy for cross and longitudinal sections, paying special attention to solidification mode and growth morphology. The width of the zone with an equiaxed growth was measured by light microscope.

The Ferrite Number (FN) of each weld was determined using a Magne-Gage calibrated according to the procedure AWS A 4.2-74.

Table 2—Test Welding Conditions

Method	Single electrode GTAW
Technique	Mechanized stringer bead
Groove	None
Filler metal	None
Welding position	Flat
Polarity	DCSP
Arc length	2 mm (0.08 in)
Electrode	EWTh-2, 2.4 mm (0.094 in.) diameter and 60 deg cone angle
Arc shielding gas	99.99% Ar, flow rate 8 L/min (17 cfh)
Root shielding gas	99.99% Ar, flow rate 8 L/min (17 cfh)
Trailing shielding gas	99.99% Ar, flow rate 8 L/min (17 cfh)
Welding torch	Vertical; orifice diameter – 11 mm (0.43 in.); distance from the sheet – 10 mm (0.39 in.)

Results

Solidification and Microstructure of the Welds

The solidification modes of the welds were assessed on the basis of the microstructure (Refs. 3, 10, 11) – Fig. 1. Sheets 1 to 8 ($Cr_{eq}/Ni_{eq} < 1.50$) solidified in a primary austenitic mode and sheets 13 to 19 ($Cr_{eq}/Ni_{eq} > 1.55$) in a primary ferritic mode with both welding speeds. Sheets 9 to 12 ($1.50 < Cr_{eq}/Ni_{eq} < 1.55$) solidified in a primary ferritic mode at 200 mm/min (8 ipm) and in a primary austenitic mode at 800 mm/min (31 ipm).

The growth morphology of all the welds was mainly columnar dendritic. In many welds, however, an equiaxed dendritic zone was found at the center line of the weld – Fig. 1B. Normally this was not continuous but took the form of islands near the weld or root faces. The equiaxed zone was found more fre-

quently at the higher welding speed. The maximum width of the equiaxed zone at the welding speed 800 mm/min (31 ipm) as a function of a sulfur content is presented in Fig. 2. It can be seen that its width increased with sulfur content; however, it did not seem to be affected by the solidification mode or phosphorus content.

The last regions to solidify in the equiaxed zone (Figs. 1C and D) etched more strongly than those in the columnar zones. This suggests more pronounced segregation. This difference was most prominent in the welds that had solidified in a primary ferritic solidification mode.

The ferrite numbers of the welds are given in Fig. 3 as a function of the ratio of chromium and nickel equivalents. The ferrite content in the welds that solidified in a primary ferritic mode decreased about 2 FN due to speed change from 200 to 800 mm/min (from 8 to 31 ipm). However, ferrite in the welds solidified in primary austenitic mode was not affected. As suggested in Fig. 3, the room temperature ferrite content corresponding to the change in solidification mode is 3 to 5 FN for Type 316 stainless steel sheets.

Weld Discontinuities

Different kinds of discontinuities were observed, depending on the welding conditions. These were cracks, center cavities, cracked center cavities, ripple cavities and undercuts. Cracks and ripple cavities were defects typical of the lower welding speed, while center cavities, their cracked versions and undercuts were mostly formed at the higher welding speed used.

Table 3 shows the typical locations, sizes, amounts and shapes of the discontinuities and also the values for the welding conditions and weld metal composi-

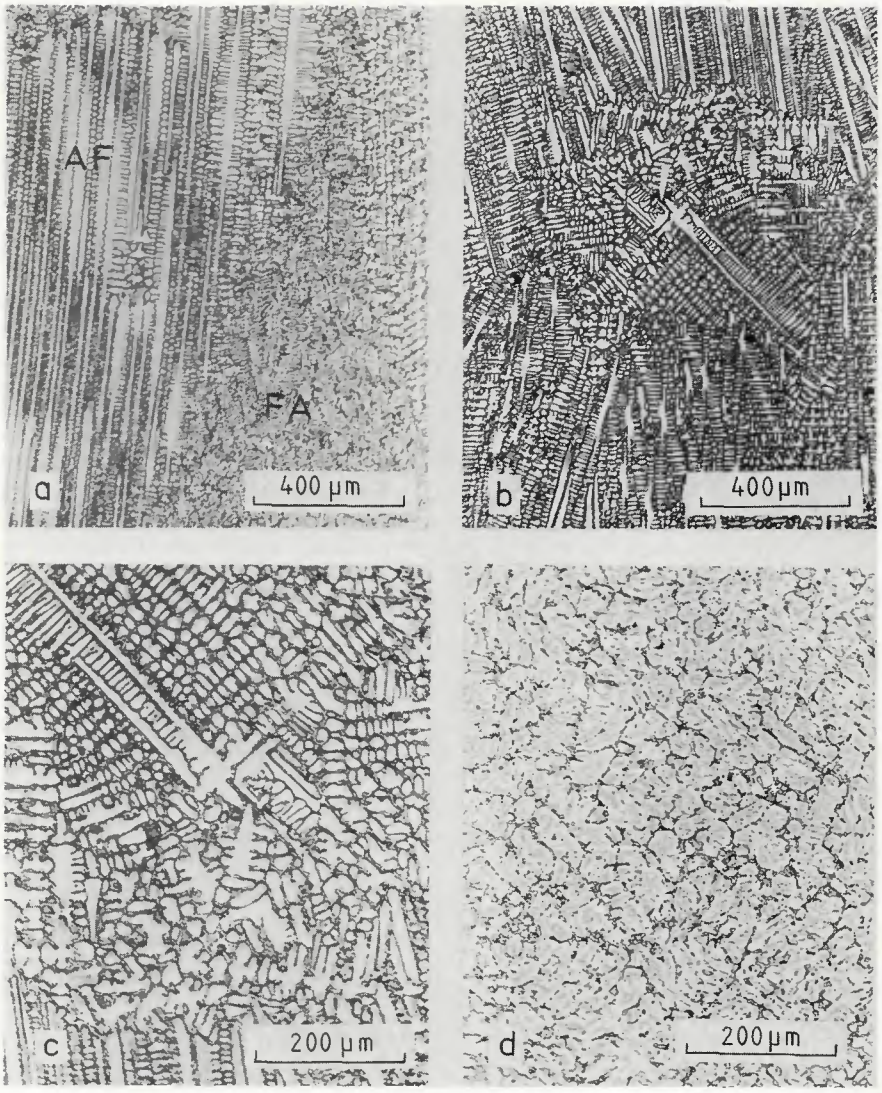

Fig. 1 – Weld microstructures: A – primary austenitic (AF) and primary ferritic (FA) solidification modes in the same weld; B, C and D – equiaxed dendritic zone near the center line of the weld in primary austenitic solidification mode (B and C) and in primary ferritic solidification mode (D). Etchant: 60% HNO_3

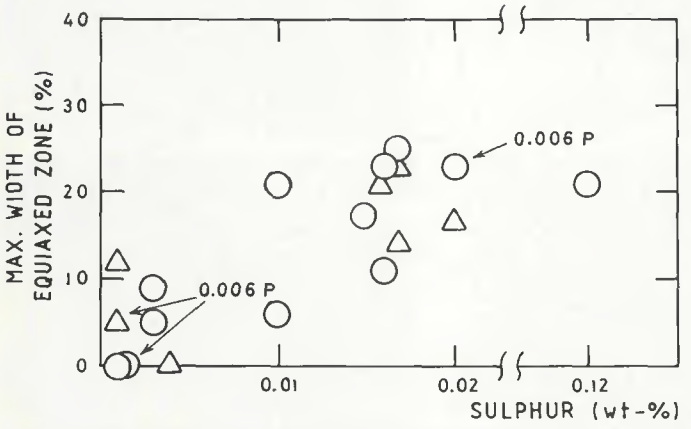

Fig. 2 – Relationship between maximum width of weld equiaxed zone and sulfur content at a welding speed of 800 mm/min (31 ipm). Circles designate primary austenitic solidification mode; triangles designate primary ferritic solidification mode

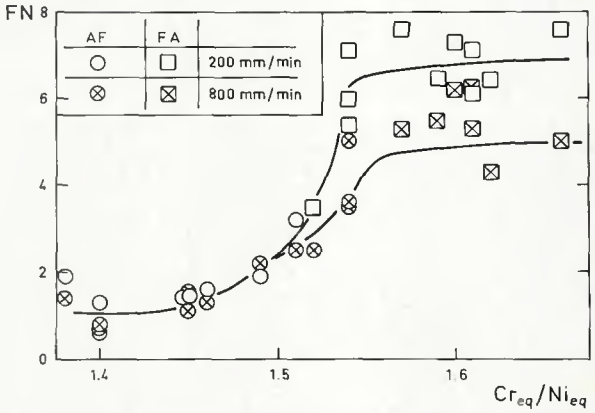

Fig. 3 – Room temperature Ferrite Number (FN) as a function of Cr_{eq}/Ni_{eq}. AF = primary austenitic solidification mode; FA = primary ferritic solidification mode

Table 3—The Typical Locations, Size, Amount and Shape of the Discontinuities and Conditions Under Which They Normally Can Be Formed[a]

	Crack	Center cavity	Cracked center cavity	Ripple cavity	Undercut	Hump
Location:						
Macrosc.	Center line	Center line	Center line	Ripple line	Weld interface	Whole width of weld
Microsc.	Last melt	Last melt	Last melt	Last melt	No correlation	No correlation
Max. length, mm	3	1	1	0.05	>250	5
Max. depth, mm	0.5	0.3	0.3	0.2	0.6	1
Max. number/mm	2	4	4	30	–	0.2
Shape	Sharp-edged	Round-edged	Round-edged, crack in bottom	Round-edged	Round-edged, flat	Round-edged
Typical conditions:						
Welding speed (mm/min)[b]	50–40	>400	400–800	<400	>600	>900
Welding current	High	High	High	High	High	Low
Cr_{eq}/Ni_{eq}	<1.50	–	–	–	–	–
Sulfur and phosphorus	P + S > 0.03% S > 0.003%	S > 0.003%	S > 0.003%	S > 0.003%	–	–

(a) This table is based on information from the literature (Ref. 2) and on data originating with this paper.
(b) 1 mm/min = 0.04 ipm.

tions at which they are normally formed. A detailed description of the defects is presented in the literature (Ref. 2). Humps observed in Ref. 2 were not found in this study, since the welding conditions used here were not typical of conditions leading to their formation.

The cracks and center cavities were always located near the center line and the ripple cavities on the ripple lines of the weld. In terms of the microstructure, they were located at the contact of the last regions to solidify—Fig. 4. The center cavities were, without exception, located in the equiaxed zone.

Effect of Solidification Mode and Impurities

The effects of sulfur content on the measures of cracks, center cavities, cracked center cavities and ripple cavities is shown in Fig. 5 (Fig. 5B also for the effects of phosphorus content). The tendency towards crack and cavity formation increased with sulfur content. These defects were infrequent if sulfur was under 0.003%. Reduction of the phosphorus content resulted in fewer cracks and ripple cavities, but did not greatly influence center cavity formation.

The solidification mode of the weld is also noticeable in Fig. 5. It may be seen that the welds which solidified in a primary austenitic mode were susceptible both to crack formation and ripple cavity formation compared to welds which had solidified in primary ferritic mode. The number and size of center cavities did not seem to depend on the solidification mode at a welding speed 800 mm/min (31 ipm).

The relation between the total length of center cavities and the maximum width of the equiaxed zone is presented in Fig. 6. As may be seen, an increase in the width of the equiaxed zone leads to considerably greater center cavity formation.

The undercuts were formed only at the higher welding speed (800 mm/min or 31 ipm), and their maximum depths varied from 0.15 to 0.57 mm (from 0.006 to 0.022 in.). No correlation was found between their occurrence and solidification mode.

Role of Ferrite Content

The maximum depth of the cracks is

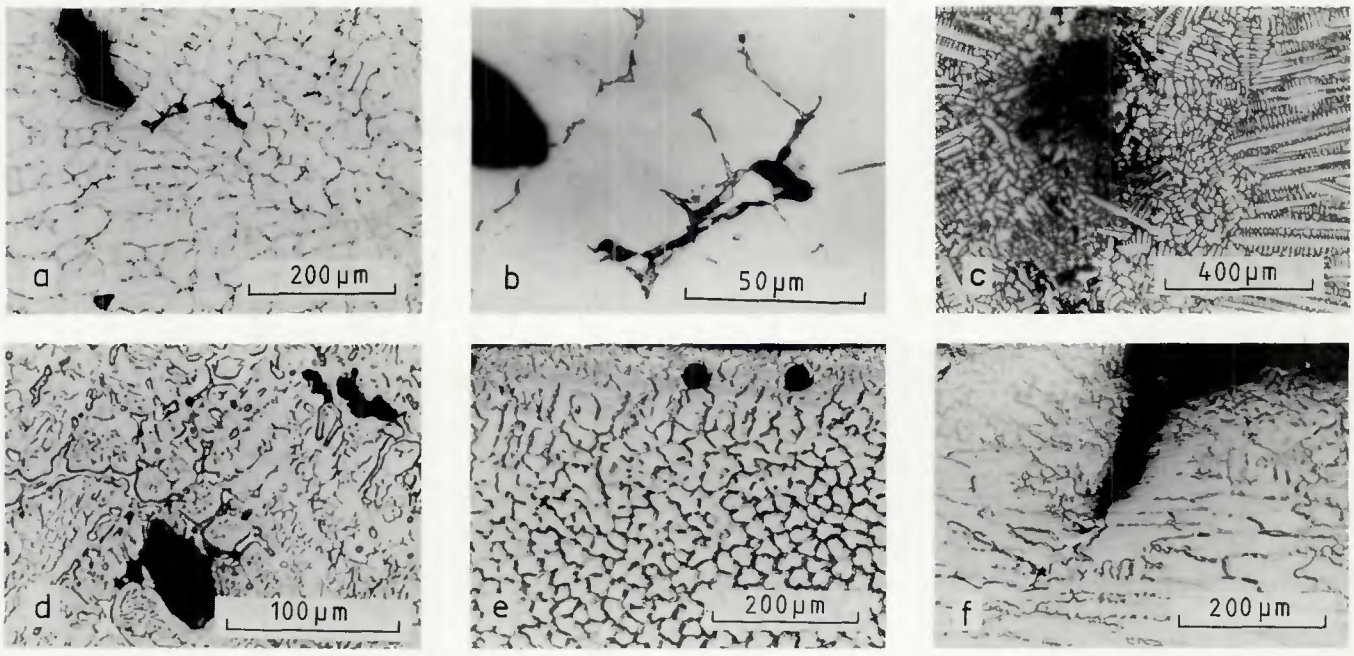

Fig. 4—Location of discontinuities in weld microstructures: A and B—cracks; C and D—center cavities; E and F—ripple cavities. Etchant: 60% HNO_3

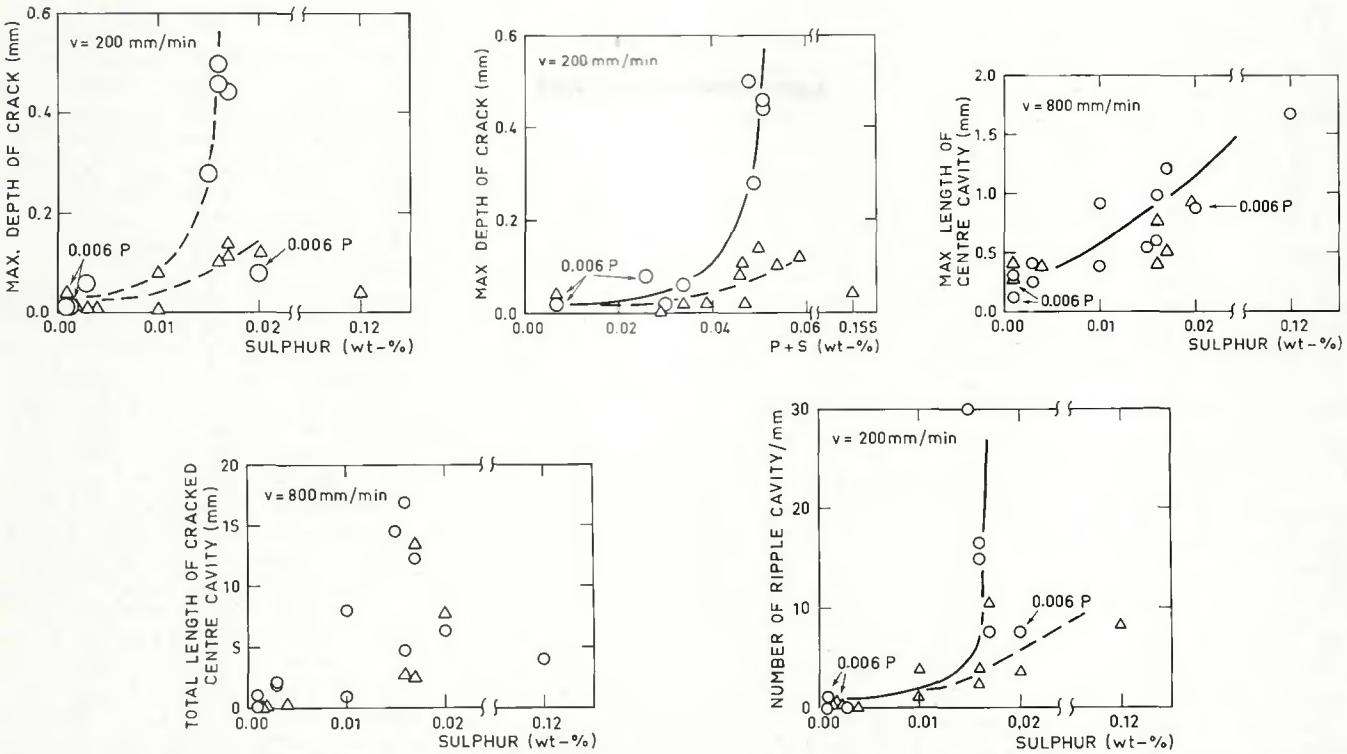

Fig. 5—Relationships between sulfur or sulfur + phosphorus content and measures for cracks, center cavities, cracked center cavities, and ripple cavities. v = welding speed; circles designate primary austenitic solidification mode; triangles designate ferritic solidification mode

shown in a P + S — FN diagram in Fig. 7A. Cracking susceptibility is seen to decrease, especially with a high impurity content, when ferrite number is over 3 FN; this corresponds to the boundary between the primary austenitic and ferritic solidification modes for Type 316 stainless steels. Welds with low impurity levels (P + S < 0.03%), were not susceptible to cracking, regardless of ferrite number.

The relation between other kinds of discontinuities and ferrite content was much weaker. The maximum length of center cavity, for instance, is seen in a sulfur-Ferrite Number diagram of Fig. 7B. The susceptibility of the weld to center cavity formation decreased with sulfur content and was not dependent on the ferrite number.

Discussion

Cracks

The cracks found in the welds studied here were evidently solidification cracks. They were located in the last regions of the welds to solidify in both the macrostructure and microstructure and were often partially backfilled, evidence that they had been in contact with the molten weld pool and had been formed during solidification.

Solidification mode was found to play an important role in cracking with a

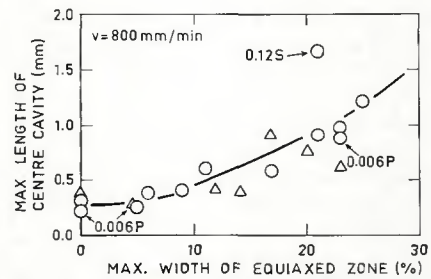

Fig. 6—Total length of center cavities as a function of the maximum width of the equiaxed zones at the welding speed of 800 mm/min (31 ipm). Circles designate primary austenitic mode; triangles designate ferritic solidification mode

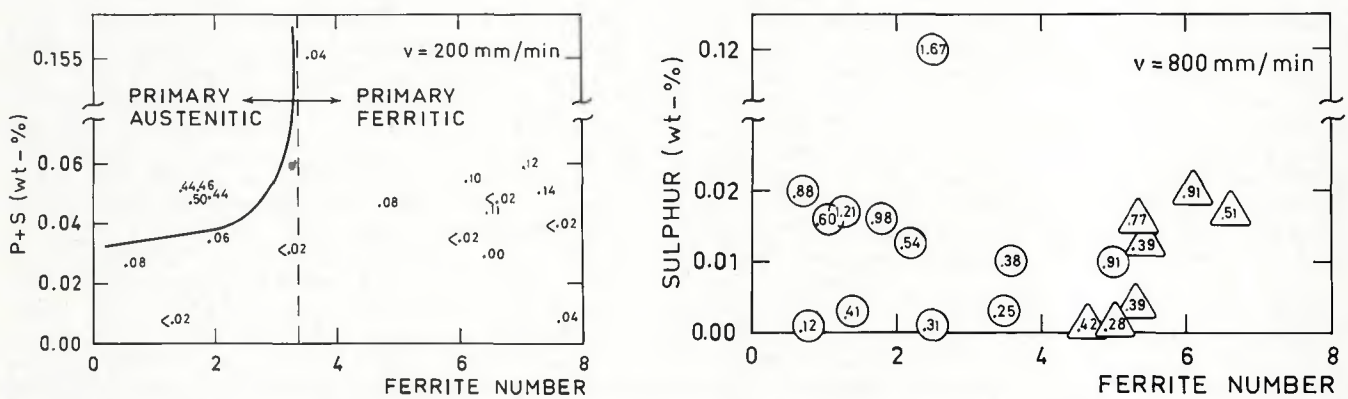

Fig. 7—Ferrite Number relationships: A—maximum crack depth in a P + S vs. FN diagram; B—maximum center cavity length in a S vs. FN diagram. v = welding speed; circles designate primary austenitic solidification mode; triangles designate primary ferritic solidification mode

normal or high impurity content. The welds solidifying in a primary austenitic mode were more susceptible to cracking than those solidifying in a primary ferritic mode—Figs. 5A and B. However, the welds with a low impurity level (*i.e.*, $P + S < 0.03\%$) were not susceptible to cracking.

These statements are supported by solidification cracking results for welds in plates of austenitic stainless steels; they show the same tendency with regard to solidification mode (Ref. 8), the limit for the impurity content simply being smaller for plates, *i.e.*, 0.01%. This is probably due to a greater rigidity in plates than in sheets, and consequently larger shrinkage stresses and strains.

According to Fig. 5A, the solidification cracking susceptibility can be forecast on the basis of sulfur content alone. If this is below 0.003%, cracks will not be formed.

The apparent effect of ferrite content on solidification cracking is actually a reflection of the effect of solidification mode. The room temperature ferrite content corresponding to the change from primary austenitic to primary ferritic solidification ranges from 3 to 5 FN for Type 316 stainless steels—Fig. 3. Consequently, the welds having a lower ferrite number (solidifying primarily as austenite) were more prone to solidification cracking than those having a higher ferrite number (solidifying primarily as ferrite)—Fig. 7A.

As discussed earlier (Ref. 12), the mechanism of formation of solidification cracks in sheets does not differ from that in plates, which has been discussed earlier (Ref. 12).

Center Cavities and Cracked Center Cavities

Pore-like discontinuities are generally classified into gas evolution and shrinkage types. The center cavities found in the present welds were shrinkage cavities formed at high temperatures. This was determined to be the case for the following reasons:

1. They had been in contact with the last melt to solidify—Figs. 4C and D.

2. As stated in another related paper (Ref. 13), their number increases with the cross section of the weld, *i.e.*, with increasing shrinkage strains.

3. As shown in the same paper, even arc shielding gases containing 17% hydrogen in argon does not cause gas evolution pores or cavities in the weld; on the other hand, Matsuda *et al.* (Ref. 14) have observed cavities of this kind in welds obtained under an argon atmosphere in a chamber evacuated to 0.13 Pa (10^{-3} mm Hg) before the test.

On the basis of Fig. 5C it was stated that center cavities grow with increasing sulfur content. This may occur for at least two reasons:

1. A higher sulfur content leads to a broader equiaxed zone—Fig. 2.; this, in turn, means a more pronounced center cavity formation—Fig. 6.

2. Sulfur segregates markedly into the molten weld pool during solidification and causes a larger mushy zone; hence the liquid films between the solidifying grains are more extensive, and the formation of shrinkage cavities is easier in welds having a high sulfur content.

The solidification mode was not found to affect center cavities or their cracked versions at a welding speed of 800 mm/min (31 ipm)—Figs. 5C and 7B. This may seem surprising, since the formation of center cavities is connected with the last melt to solidify, its composition, and the liquid films between its solidifying grains, which are normally more pronounced in the welds solidifying in a primary austenitic than in a primary ferritic mode. On the basis of differences in the etched microstructures, however, segregation in the equiaxed zones seemed to be exceptionally pronounced in welds solidifying in the primary ferritic mode and could correspond to that observed in welds solidifying in primary austenitic mode—Figs. 1C and D.

Cracks are formed preferentially at low welding speeds, while center cavities are typically found in welds made at higher speeds. Both kinds of discontinuities have been in contact with the last melt to solidify. The transition from crack to center cavity is evidently related to equiaxed zone formation with increasing welding speeds. It is hard for cracks, which require large strains for their formation, to form in the equiaxed zone, where the liquid films are divided over a larger area than in welds without an equiaxed zone. Otherwise, center cavities can form in the equiaxed zone and are, therefore, typically encountered at high welding speeds.

Other Discontinuities

The formation of ripple cavities has been discussed in the literature (Ref. 2), where it was found that these typically form at high welding currents and low speeds. The present results show that they are also influenced by the solidification mode and by impurities. Ripple cavities formed most frequently in welds which solidify in a primary austenitic mode or have a high sulfur content. These effects are based on the same facts mentioned in connection with cracks.

Undercuts were not influenced by the solidification mode. This is a finding which supports the statements discussed in the literature (Ref. 2)—namely, that their formation is basically dependent on the flow of the molten weld pool.

Practical Significance of the Results

The most important discontinuities to form in sheet and tube welding are cracks, center cavities and undercuts. The results of the investigation reported here and information in a previous paper (Ref. 2) show that cracks can be formed at low welding speeds, while center cavities and undercuts are typical of high speeds.

Cracks can be formed at the welding speeds used in connection with the single electrode GTA welding. Since cracking susceptibility is highly dependent on the solidification mode, base and filler metals that solidify primarily as ferrite ($Cr_{eq}/Ni_{eq} > 1.5$) should be used—Figs. 5A and B. The presence of impurities will then not be critical. On the other hand, if the composition of the weld metal is such that it solidifies primarily as austenite ($Cr_{eq}/Ni_{eq} < 1.5$), the impurity content should be very low, *i.e.*, $P + S < 0.03\%$, and $S < 0.003\%$—Figs. 5A and B.

The solidification mode can be controlled only in certain types of welds, *e.g.*, welds in Types 316, 317 and 309 stainless steel. With other types, a reduction in the impurity content is necessary in order to minimize crack formation.

Undercuts can be effectively eliminated at high welding speeds by the use of multiple electrode GTA welding (Ref. 13). However, center cavity formation can then be a problem. The center cavities do not seem to be affected by solidification mode; they can be minimized, however, by reducing the sulfur content to below 0.003%—Fig. 5C.

Weld discontinuities can also be influenced by welding conditions and shielding gas composition as shown elsewhere (Refs. 2 and 13).

Conclusions

Defect formation was investigated in nineteen Type 316 austenitic stainless steel sheets. Single electrode autogenous GTA welding was used at welding speeds 200 and 800 mm/min (8 and 31 ipm). The compositions of the welds varied within the limits $Cr_{eq}/Ni_{eq} = 1.38$ to 1.66, where $Cr_{eq} = \%Cr + 1.37\% Mo + 1.5\% Si + 2\% Nb + 3\% Ti$ and $Ni_{eq} = \%Ni + 0.31\% Mn + 22\% C + 14.2\% N + \%Cu$ and impurities in the limits $S = 0.001$ to 0.12% and $P = 0.006$ to 0.038%. The results allow the following conclusions to be made:

1. Several types of discontinuities can be formed during welding: cracks, center cavities, cracked center cavities, ripple cavities, and undercuts.

2. Crack formation is mostly affected by the solidification mode, more and deeper cracks being formed in welds solidifying primarily as austenite ($Cr_{eq}/$

$Ni_{eq} < 1.5$) than in welds solidifying primarily as ferrite ($Cr_{eq}/Ni_{eq} > 1.5$). The effect of solidification mode on ripple cavities is similar, although very much fainter. Center cavities, cracked center cavities, and undercuts are not influenced by solidification mode.

3. Sulfur and phosphorus also have their effects on discontinuity formation. The formation of cracks, center cavities, cracked center cavities and ripple cavities is markedly less when the sulfur content is below 0.003%. Phosphorus has a same kind of effect on cracking, but its effect on the other kinds of discontinuities is less noticeable.

4. Shrinkage is the main reason for crack and cavity formation. The transition from cracks to center cavities is connected with the formation of an equiaxed zone in the welds at high welding speeds.

Acknowledgments

Support from the Foundation of Outokumpu Oy and the Academy of Finland is gratefully acknowledged. The author also thanks Mr. M. Hicks, M. A., for revising the English language of the manuscript.

References

1. Oyler, G. W., Matuszek, R. A., and Garr, C. R. 1967. Why some heats of stainless steel may not weld. *Welding Journal* 46 (12):1006–1011.

2. Kujanpää, V. 1983. Weld defects in austenitic stainless steel sheets—Effect of welding parameters. *Welding Journal* 62 (2):45-s to 52-s.

3. Suutala, N., Takalo, T., and Moisio, T 1979. Relationship between microstructure and solidification in austenitic stainless steel welds. *Metallurgical Transactions* 10A (4): 512–514.

4. Suutala, N. Effect of solidification conditions on the solidification mode in austenitic stainless steels. 1983. *Metallurgical Transactions A.* 14A(2): 191–197.

5. Hammar, Ö., and Svensson, U. 1979. Influence of steel composition on segregation and microstructure during solidification of austenitic stainless steels. *Proc. Conf. Solidification and Casting of Metals.* ed. J. Hunt: 401–410. London: The Metals Society.

6. Suutala, N. Effect of manganese and nitrogen on the solidification mode in austenitic stainless steel welds. 1982. *Metallurgical Transactions A.* 13A(12): 2121–2130.

7. Lundin, C. D., DeLong, W. T., and Spond, D. F. 1975. Ferrite-fissuring relationship in austenitic stainless steel weld metals. *Welding Journal* 54(8): 241-s to 246-s.

8. Kujanpää, V. P., Suutala, N. J., Takalo, T. K., and Moisio, T. J. I. 1980. Solidification cracking—estimation of the susceptibility of austenitic and austenitic-ferritic stainless steel welds. *Metal Construction* 12 (6):282–285.

9. Gooch, T. G. 1976. Ferrite and weld metal cracking in stainless steel. *The Welding Institute Research Bulletin* (9): 227–231.

10. Takalo, T., Suutala, N., and Moisio, T. 1979. Austenitic solidification mode in austenitic stainless steel welds. *Metallurgical Transactions* 10A (8): 1173–1181.

11. Suutala, N., Takalo, T., and Moisio, T. 1980. Ferritic-austenitic solidification mode in austenitic stainless steel welds. *Metallurgical Transactions* 11A (5): 717–725.

12. Kujanpää, V., Suutala, N., Takalo, T., and Moisio, T. 1979. Correlation between solidification cracking and microstructure in austenitic and austenitic-ferritic stainless steel welds. *Welding Research International* 9 (2): 55–77.

13. Kujanpää, V. P., Karjalainen, L. P., and Sikanen, H. A. V. 1983. Role of shielding gases in discontinuity formation in GTA welding of austenitic stainless steel strips. *Welding Journal* 63(5): 151-s to 155-s.

14. Matsuda, F., Hashimoto, T., and Senda, T. 1969. Fundamental investigations on solidification structure in weld metal. *Transactions of NRIM* 11 (1):89–104.